Optimal Power Scheduling for a Grid-Connected Hybrid PV-Wind-Battery Microgrid System

Hernández, Adriana Carolina Luna; Aldana, Nelson Leonardo Diaz; Savaghebi, Mehdi; Quintero, Juan Carlos Vasquez; Guerrero, Josep M.; Sun, Kai; Chen, Guoliang; Sun, Libing

Published in:
Proceedings of the 31st Annual IEEE Applied Power Electronics Conference and Exposition (APEC)

DOI (link to publication from Publisher):
10.1109/APEC.2016.7468025

Publication date:
2016

Document Version
Early version, also known as pre-print

Optimal Power Scheduling for a Grid-Connected Hybrid PV-Wind-Battery Microgrid System

Adriana Luna
Nelson Diaz
Mehdi Savaghebi
Juan C. Vasquez
Josep M. Guerrero
Department of Energy Technology
Aalborg University, Aalborg, Denmark
Email: acl@et.aau.dk, nda@et.aau.dk,
mes@et.aau.dk, juq@et.aau.dk, joz@et.aau.dk
http://www.microgrids.et.aau.dk

Kai Sun
Tsinghua University
Tsinghua, China
Email: sun-kai@mail.tsinghua.edu.cn

Guoliang Chen
and Libing Sun
Shanghai Solar Energy
& Technology Co., Ltd.

***Abstract*—In this paper, a lineal mathematical model is proposed to schedule optimally the power references of the distributed energy resources in a grid-connected hybrid PV-wind-battery microgrid. The optimization of the short term scheduling problem is addressed through a mixed-integer linear programming mathematical model, wherein the cost of energy purchased from the main grid is minimized and profits for selling energy generated by photovoltaic arrays are maximized by considering both physical constraints and requirements for a feasible deployment in the real system. The optimization model is tested by using a real-time simulation of the model and uploaded it in a digital control platform. The results show the economic benefit of the proposed optimal scheduling approach in two different scenarios.**

I. Introduction

A microgrid is an aggregation of distributed energy resources (DER) such as renewable energy sources (RES), loads and energy storage systems (ESS) as controllable entities which may operate in grid-connected or islanded mode. Hierarchical operation has been defined in order to standardize the control of the microgrid. In this sense, primary, secondary and tertiary controllers have been defined in order to provide adequate voltage and current regulation (primary control), restoring any steady-state error introduced by primary control (secondary control), and regulate the power flow between DER or between several clusters of microgrids (tertiary control) [1]. On top of that an Energy Management System (EMS) defines set points for the previous control layers in order to achieve optimal dispatch regarding specific objectives and limits generation capacity when is in islanded mode or power exchange with the utility grid while operates in grid-connected mode, buying and selling the shortage or surplus of power to or from the main grid [2].

A full-scale demonstrative, research-oriented microgrid has been installed in Shanghai, China for evaluating the performance of several EMS strategies, oriented to optimize the operation of the microgrid by scheduling the power of the distributed energy resources (Fig. 1) [1] (www.meter.et.aau.dk). The proposed EMS aims to minimize the cost of buying energy from the main grid and maximize the revenue due to the photovoltaic (PV) energy generation, while preserving the lifetime of the ESS based on batteries by avoiding overcharge, excessive discharge and discharge cycles. In this proposal, a mixed integer linear programming (MILP) model is used in order to obtain an optimal power dispatch regarding economic issues. The proposed optimization model can be deployed easily in real microgrids sites since it is linear, simple and can be synthesized in commercial optimization software such as GAMS. This fact is a remarkable advantage compared to others optimization strategies [2] [4, 5].

II. Microgrid Description

The system under test is a 200 kW PV-wind-battery microgrid (Fig. 2). For the case study presented in this paper, the microgrid will operate connected to the main grid. Because of that, the main grid impose the voltage and frequency conditions at the point of common coupling. Meanwhile, all the inverters will operate in current control mode as grid-following units [3].

The microgrid is composed by 6 PV generators all of them will operate by following local maximum power point tracking (MPPT) strategies. On top of that, the EMS schedules the startup or shutdown signals for PV generators. On the contrary, the two wind generators can operate in interactive and non-interactive way since their power generation may be curtailed from the EMS [4].

Moreover, in order to enhance the performance of the ESS based on batteries a two stage procedure which avoids battery overcharge is recommended by the battery manufacturers. Therefore, the battery control should be complemented with a voltage-limiting strategy. In this case, the ESS has two control operation modes: limited current charge and constant voltage charge. At the first stage, the ESS is charged based in the power reference defined by the EMS. It is important to say that the EMS considers maximum power ratings of the ESS in order to limit the battery current. On the other hand, the second stage (constant voltage charge) is activated once the battery array reach a threshold value. At this stage, the ESS

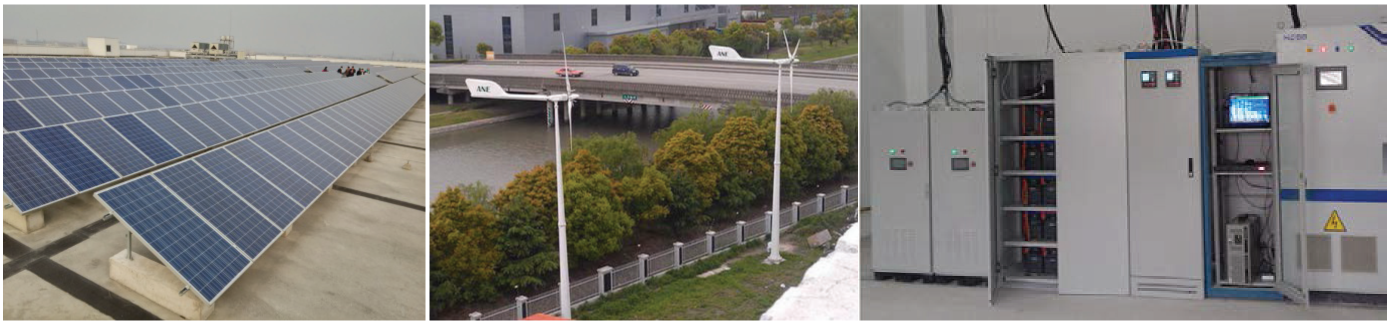

Fig. 1. Real site microgrid in Shanghai-China.

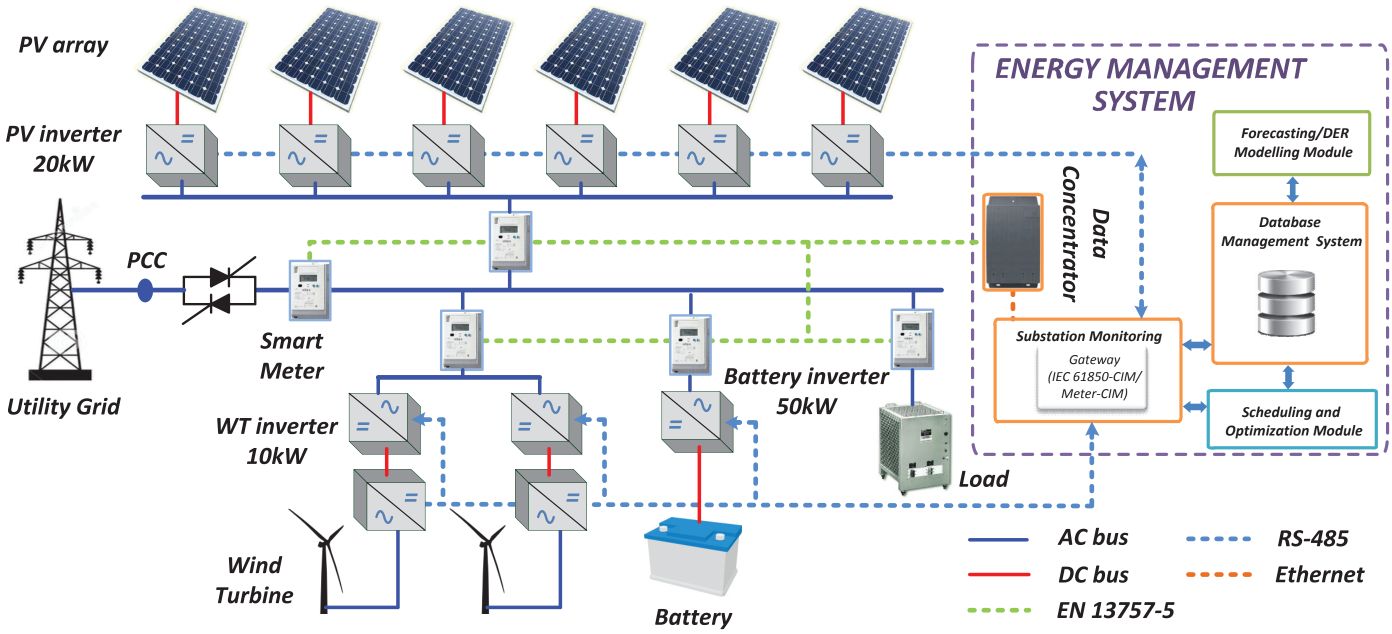

Fig. 2. Scheme of the microgrid.

only takes from the microgrid as much power as it needs in order to keep the battery voltage in a constant value [5], [4].

Another important point is to avoid excessive discharge of the battery. At this sense, the state of charge (SoC) of the battery is restricted to 50% for ensuring larger life-time of the battery array [5], [6]. For achieving this objective the EMS should ensure proper scheduling of the other distributed energy resources including the main grid in order to get an optimal commitment between battery charge and the energy bought from the grid. Additionally, the EMS optimizes the operation of the system in order to reduce the number of discharging cycles. Also, the microgrid supplies a local resistive load of 5 kW.

Apart from that, the microgrid is complemented with a EMS which schedules the operation of the distributed energy resources by considering optimal operational objectives [2]. The proposed EMS has been designed as a modular architecture in which each module performs different functions independently and exchanges information through the database system, as can be seen in Fig. 2. In this paper we will presented specifically the model implemented in the *scheduling and optimization module*.

TABLE I. SETS OF THE OPTIMIZATION MODEL

Name	Description	Definition
t	discrete time slot	$\{1, 2, \ldots T\}$
i	PV units	$\{PV1, PV2, \ldots, PV6\}$
j	WT units	$\{WT1, WT2\}$

III. OPTIMIZATION PROBLEM

In this proposed approach, a Mixed Integer Linear Programming (MILP) problem is defined in order to minimize the cost of buying energy from the utility grid and maximize the revenue obtained by selling energy generating by the PVs.

A. Statements

The indexes, parameters and variables used in this model are summarized in tables I, II and III, respectively and will be presented during the description of the model.

The optimization problem is formulated assuming discrete time representation [7]. Thereby, the time horizon corresponds to $T * \Delta t$. Additionally, the values of the power are considered equal to the average value for each time interval and have been scaled in per units (p.u.) with S_{base} as the base.

TABLE II. PARAMETERS OF THE MODEL

Name	Description	Value
T	Number of time slots	24 (h)
Δt	Duration of interval	1 (h)
n_i	Number of PV arrays	6
n_j	Number of WT	2
$C_{sell}(t)$	Cost of selling energy	1.147 (Yuan/kWh)
$C_{buy}(t)$	Cost of buying energy (night)	0.307 (Yuan/kWh)
	Cost of buying energy (day)	0.617 (Yuan/kWh)
$P_{PV_{max}}(i,t)$	Max power for PV arrays	
	for $i = \{PV1$ to $PV4\}$	0.733 (p.u.)
	for $i = \{PV5, PV6\}$	0.585 (p.u.)
$P_{WT_{max}}(j,t)$	Max WT power $\forall j$	0.3923 (p.u.)
$P_L(t)$	Power required by the load	0.1 (p.u.)
$P_{bat_{max}}$	Maximum power of battery	1 (p.u.)
$P_{bat_{min}}$	Minimum power of battery	-1 (p.u.)
$P_{grid_{max}}$	Max. power bought from utility	1 (p.u.)
S_{base}	Scaled base	5 kW
SoC_{max}	Maximum SoC	100 (%)
SoC_{min}	Minimum SoC	50 (%)
$SoC(0)$	Initial Condition of SoC	70 (%)
Cap_{bat}	Capacity of the battery	1 p.u.
χ	Penalty cost to the battery	$C_{buy}(t) * 0.1$(Yuan/kWh)

TABLE III. VARIABLES OF THE MODEL

Name	Description
Decision variable	
$Totalcost$	Objective function
Scheduled variables	
$X_{PV}(i,t)$	ON/OFF commands for PV arrays
$P_{WT}(j,t)$	Power of the WTs
$P_{bat}(t)$	Power of the battery
$P_{buy}(t)$	Power bought from the utility
$P_{sell}(t)$	Power sold to the utility
Auxiliar variables	
$X_{grid}(t)$	Status bought/sold
$SoC(k,t)$	State of charge

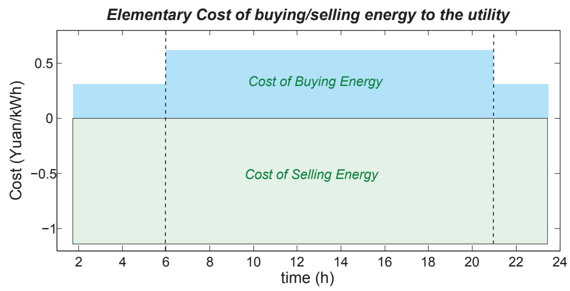

Fig. 3. Elementary costs of buying and selling energy to the utility in Shanghai [8]

On the other hand, the cost of buying for microgrids in Shanghai [8] is established in a time of use (ToU) scheme where the consumers is persuated to change its consumption behavior by means of fixed differentiate tariff during the day and the night (Fig. 3). Additionally, the grid company only buys energy generated by PV arrays, so the generation provided by WT can be used just for local demand.

B. Definition of the Model

This proposal aims to minimize the cost of buying energy from the utility grid and maximizing the revenue obtained by generating energy from the PVs. In this way, the following objective function has been defined,

$$\begin{aligned} Totalcost = &\sum_{t=1}^{T} \{P_{buy}(t) * \Delta t\} * C_{buy}(t) \\ &- \sum_{t=1}^{T} \{P_{sell}(t) * \Delta t\} * C_{sell}(t) \\ &+ \sum_{t=1}^{T} \left[\frac{SoC_{max} - SoC(t)}{100} \right] * \chi \end{aligned} \tag{1}$$

The first two terms in 2 fulfills the requirements of the optimization problem for the time horizon. Additionally, the third term is included as a penalty for not charging the battery in order to take advantage of the surplus energy that should be curtailed.

The constraints of the optimization problem start with the energy balance.

$$\begin{aligned} &\{P_{buy}(t) * \Delta t - P_{sell}(t) * \Delta t\} + \\ &\sum_{i=1}^{n_i} X_{PV}(i,t) * P_{PV_{max}}(i,t) * \Delta t + \\ &\sum_{j=1}^{n_w} P_{WT}(j,t) * \Delta t + P_{bat}(t) * \Delta t = P_L(t) * \Delta t \end{aligned} \tag{2}$$

The first two terms are related to the energy absorbed from the grid and injected to the grid respectively. In turns, the third expression is the energy provided by the PV arrays. In this case, the variable $X_{PV}(i,t)$ allows to manage the energy by sending ON/OFF commands. The next term corresponds to the energy supplied by the WT. After that, the energy of the battery is included. To complete the balance, the energy required by the load has to equal to the addition of the previous expressions.

The boundaries related to the power of the WTs are,

$$0 < P_{WT}(j,t) < P_{WT_{max}}(j,t) \tag{3}$$

Regarding the utility, the constraints are,

$$0 \leq \quad P_{buy}(t) \quad \leq P_{grid_{max}}(t) * X_{grid}(t) \tag{4}$$

$$0 \leq \quad P_{sell}(t) \quad \leq \sum_{i=1}^{n_i} P_{PV_{max}}(i,t) * (1 - X_{grid}(t)) \tag{5}$$

Besides, the constraints related to the battery are

$$SoC(t) = SoC(t-1) - \varphi * P_{bat}(t) * \Delta T \tag{6}$$

$$\sum_{t=1}^{T} SoC(t) - SoC(t-1) > 0 \tag{7}$$

$$SoC_{min} < SoC(t) < SoC_{max} \tag{8}$$

$$P_{bat_{min}} < P_{bat}(t) < P_{bat_{max}} \tag{9}$$

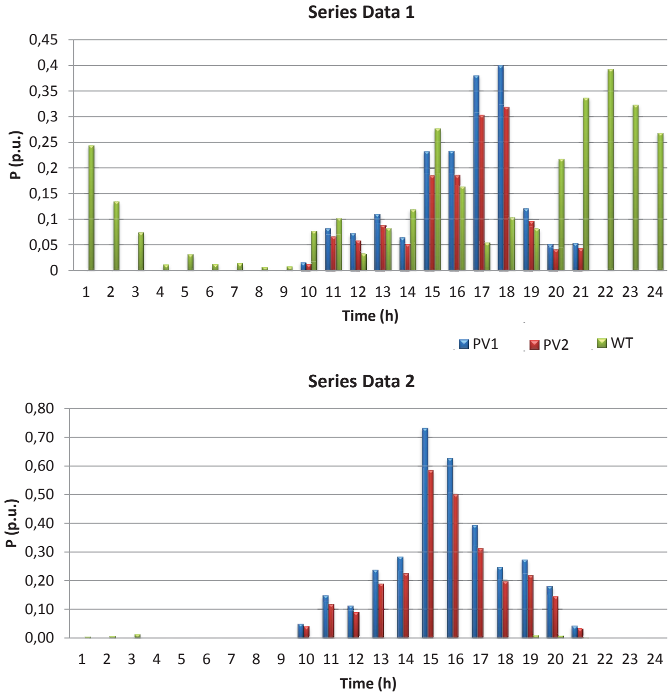

Fig. 4. RESs series data. Top to down: scenario 1 (average RESs generation) and scenario 2 (low WT generation and high PV generation).

IV. Results

A. Scheduling Results

The software GAMS is used as algebraic model language which configures the use of the solver CPLEX in order to compute the power references obtained for the proposed MILP. The optimization model is run assuming an initial condition of SoC of 70%. Additionally, two scenarios of RES generation are considered as shown in Fig. 4, with an average and a low WT generation. In the figure, the profile *PV1* corresponds to the generation of the arrays PV1 to PV4, while the profile *PV1* is the one of the arrays PV5 and PV6, and the profile *WT* is the same for WT1 and WT2.

1) Scenario 1. Average generation: The scheduled variable related to the PV arrays is shown in Figs. 5. As can be seen, the arrays are not turned off during the day at any time since this energy is sold to the grid at good price, and they are disconnected during the night because there are no generation at that times.

Figure 6 presents the WT power profile. As can be seen, there are surplus of energy during the day and just part of the energy is used while some curtailment is deployed.

On the other hand, the profiles of selling and buying power to the utility are shown in Fig. 7 and 8. It is possible to see in Fig. 7 that all the generated PV energy is sold to the utility whereas Fig. 8 shows that the local generation is enough to supply the load and thus, it is not needed to buy energy from the grid.

Regarding the battery, the scheduled power profile and the consequently SoC are presented in Figs. 9 and 10. As can be seen, the battery is discharged when the power provided for

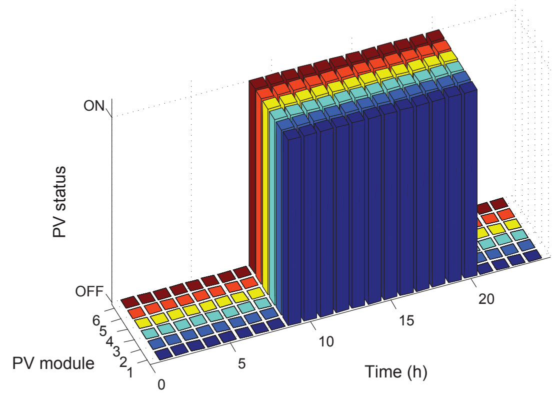

Fig. 5. Scheduled ON/OFF commands for PV modules.

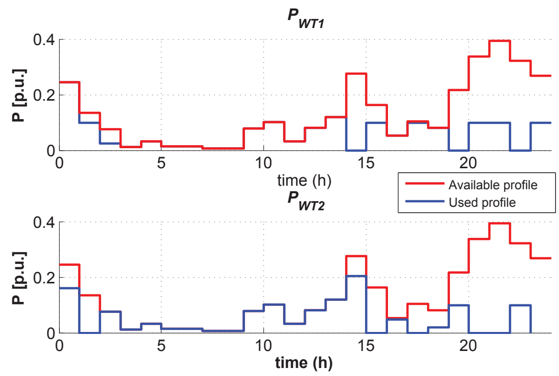

Fig. 6. Power references for WTs in scenario 1. Red line: available power. Blue line: Used power

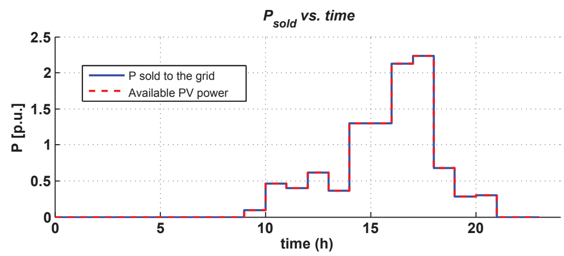

Fig. 7. Scheduled power sold to the utility in scenario 1. Red dashed line: available PV power, Blue solid line: scheduled power to be sold to the utility

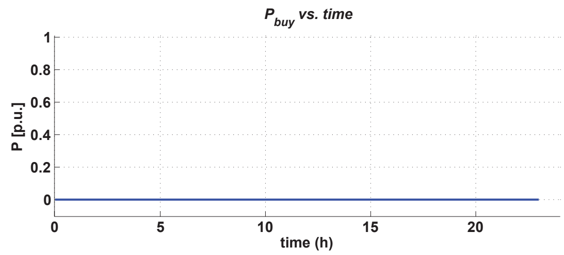

Fig. 8. Scheduled power bought from the utility in scenario 1

the WT is low while it is charged when there is high power in the WT.

2) Scenario 2. Low WT generation and High PV generation: In this case the PV profile for the PV array is identical

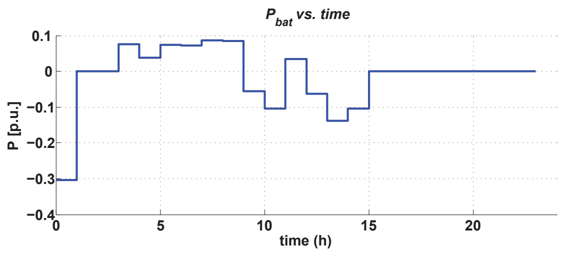

Fig. 9. Scheduled power of the battery in scenario 1

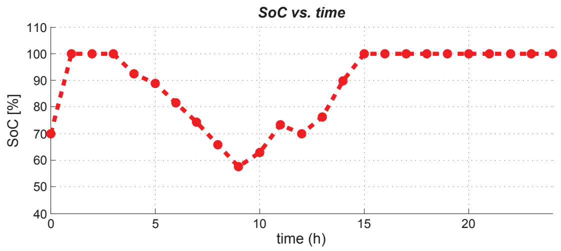

Fig. 10. Expected State of Charge of the battery in scenario 1.

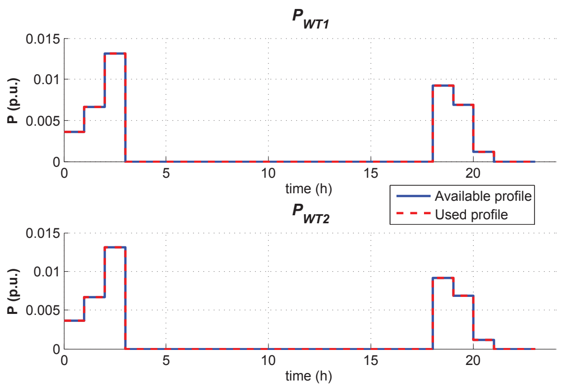

Fig. 11. Power references for WTs in scenario 2. Red dashed line: Used power. Blue solid line: available power

to the previous case (see Fig. 5) since the energy produced by the PV can be sold to the utility without restrictions.

On the other hand, the scheduled profile of the WT is presented in Fig. 11. It is possible to see that in this scenario there is no surplus of energy, so it is not required to curtail energy at any time during the day.

Regarding the utility, the profiles of selling and buying energy are shown in Fig. 12 and 13. As can be seen, part of the energy generated by the PV arrays is used in the local consumption and, at the same time, it is required to buy energy from the utility because the energy provided by the WT is not enough to supply the demand.

Additionally, the scheduled power profile and the expected SoC of the battery are presented in Fig. 14 and 15, respectively.

Note that, the optimization model schedules to buy energy during the time when the elementary cost of buying energy from the main grid is lower, rather than using the energy available in the battery. After that, the scheduling hold charged the battery to use the energy at the end of the day when the

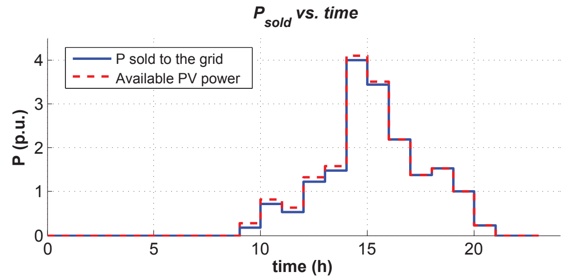

Fig. 12. Scheduled power sold to the utility in scenario 2. Red dashed line: available PV power, Blue solid line: scheduled power to be sold to the utility

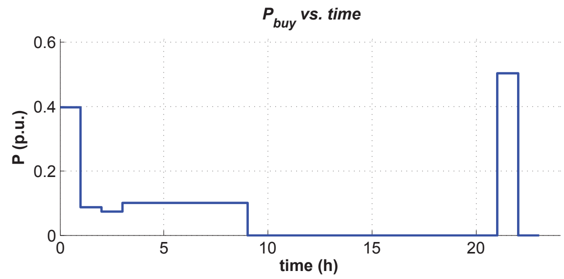

Fig. 13. Scheduled power bought from the utility in scenario 2

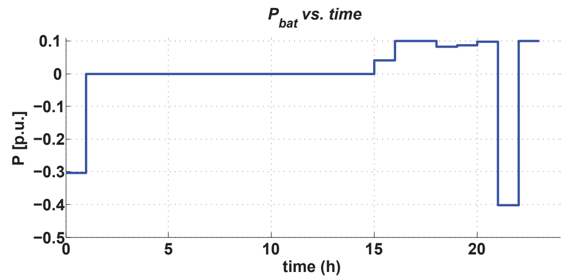

Fig. 14. Pbat

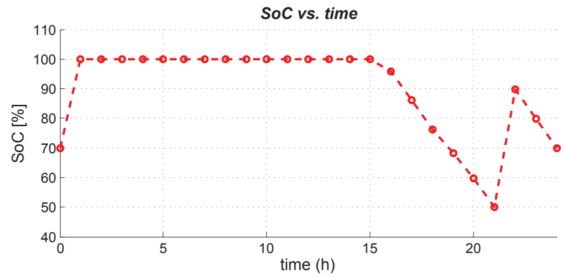

Fig. 15. Expected State of Charge of the battery in scenario 2.

PV arrays do not generate energy.

Finally, Table IV summarizes the revenue for the user in each case in which negative values indicate earning money and positive values mean must pay money. It is possible to see that for average generation it is expected profits of 582 Yuan in one day. Also, when there is high generation of PV, the user gets more profits even in this case when it is required to buy energy during some times during the day due to the low power generation by WTs.

TABLE IV. REVENUE FOR THE USER (COST FOR BUYING MINUS COST FOR SELLING)

Scenario	Cost (Yuan)
S 1 (Average generation)	-582.81
S 2 (High PV and low WT generation)	-995.97

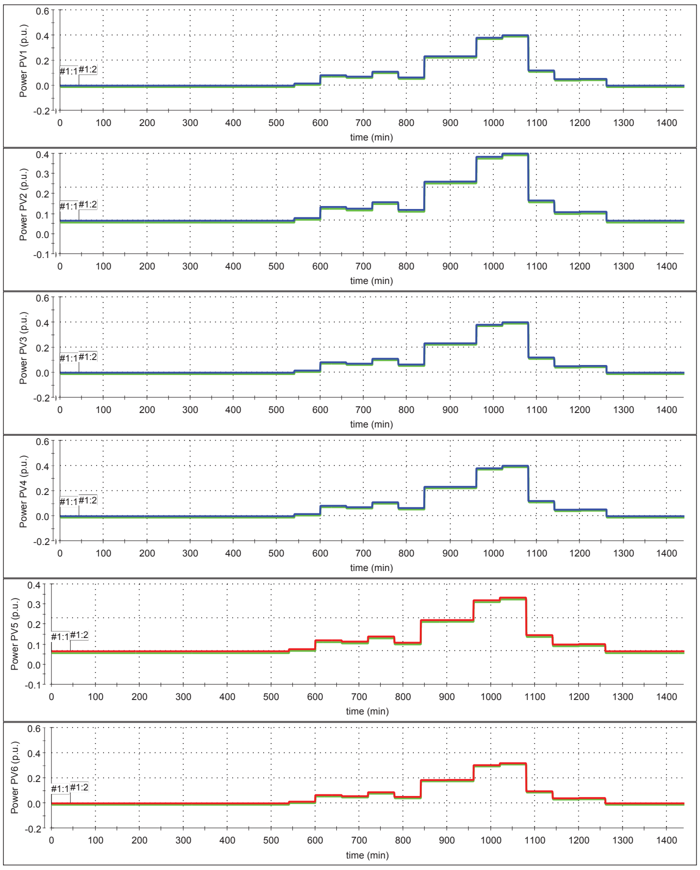

Fig. 16. Power profile of each PV array in real-time simulation considering scenario 1. Top to bottom: PV1 to PV6 power profiles. From PV1 to PV4: blue line: available power, green line: used power. For PV5 and PV6: red line: available power, green line: used power

B. Real time simulation

In order to test the proposed optimization model, a real time simulation of the microgrid is deployed considering the case study. To be more precise, the obtained results are included in a detailed Simulink model of the microgrid and subsequently uploaded in a digital control platform in one of the setups at the Research Microgrid Laboratory of Aalborg University[9].

To deploy the simulation of one day, the data were time-scaled i.e. one hour corresponds to one minute simulation. In the same way, the capacity of the battery and the elementary cost of the grid were scaled. The real time simulation is performed by using average values of available power in deterministic scenarios in order to test the performance of the optimization model.

1) Scenario 1. Average generation: The real time simulation results related to the first scenario are presented in Fig. 16, 17, 18, 19 and 20.

The available and used power profile of the PV arrays are

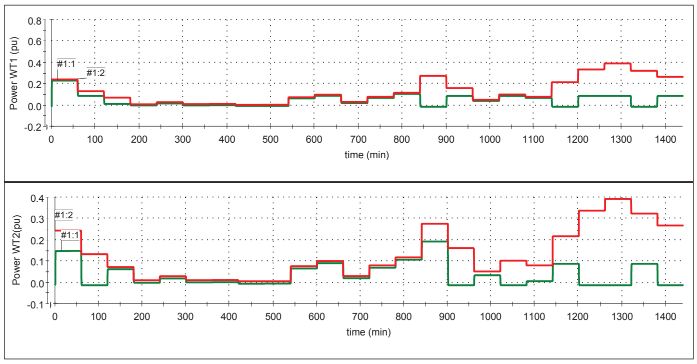

Fig. 17. Power profile of each WTs in real-time simulation considering scenario 1. Red line: available power, green line: used power

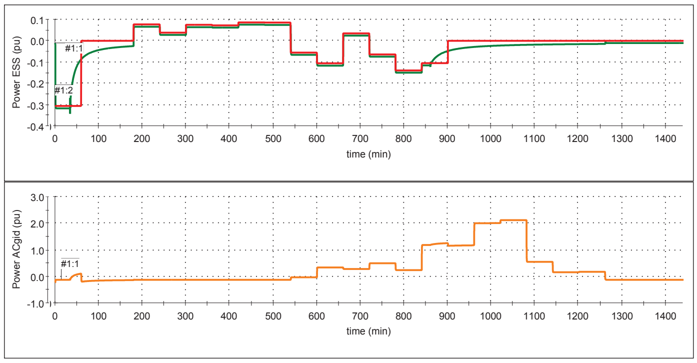

Fig. 18. Power profile of the battery and the utility in real-time simulation considering scenario 1. For battery power profile (top): scheduled profile (red line) and obtained profile (green line).

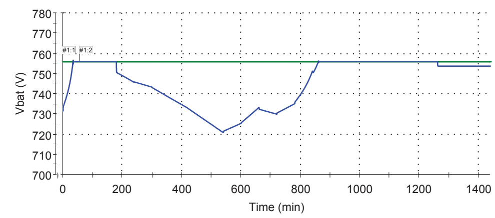

Fig. 19. Battery voltage obtained in real-time simulation considering scenario 1. Threshold voltage (green line) and battery voltage (blue line).

shown in Fig. 16. As can be seen, the first four PV arrays produce more energy (blue lines) than the next two PV arrays (red lines) since the first ones have a slighly higher power rating. Besides, the available and used profiles of each PV array are equal due to they have been scheduled to be activated during the generation hours (Fig. 5).

Meanwhile, the available and used power profile of the WT are presented in Fig. 17. It is possible to see that the powers are set to follow the scheduled profiles presented in Fig. 6, where part of the energy has been curtailed.

Regarding the battery, in the first frame of Fig. 18, in Fig. 19, and in Fig. 20 are presented the power profile, voltage and SoC, respectively.

Particularly, the first frame of Fig. 18 shows the scheduled power profile (red line) and the power profile obtained in the real-time simulation (green line) of the battery. As can be seen,

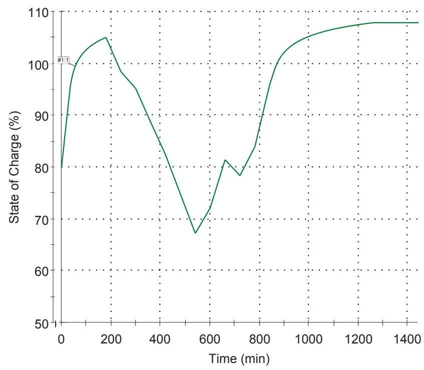

Fig. 20. SoC of the battery in real-time simulation considering scenario 1.

the battery follows the scheduled references most of the time during the day. In fact, these profiles differ when the battery voltage reaches the voltage threshold (Fig. 19) and thus, it is considered charged. In this case, the battery should control the voltage in this value to avoid damage due to over-voltage. For this reason, the battery stop following the power reference until the available energy is not enough to hold the voltage threshold. Nevertheless, the power profile keeps the tendency scheduled by the optimization model. Accordingly, the SoC of the battery (Fig. 20) are similar to the expected SoC (Fig. 10).

Moreover, the power profile exchanged with the utility is presented in the second frame of Fig. 18. In this case, the profile is positive when microgrid injects power to the grid (sells) and negative when absorbs power (buys). The behavior of this profile follows accurately the behavior expected in the optimization stage (see Fig. 7 and 8).

2) Scenario 2. Low WT generation and High PV generation: The real time simulation results related to the second scenario are presented in Fig. 21, 22, 23, 24 and 25.

As in the previous scenario, all the energy generated by the PV arrays are used as shown in Fig. 21. In turns, the power profile of the WT follows the scheduled reference without curtail available energy.

Regarding the battery, in the first frame of Fig. 23, in Fig. 24, and in Fig. 25 are presented the power profile, voltage and SoC, respectively.

The scheduled power profile (red line) and the power profile obtained in the real-time simulation (green line) of the battery are shown in the first frame of Fig. 23. It is possible to see that these profiles differ only when the battery is charged (when voltage reaches the voltage threshold in Fig. 24). Nevertheless, the power profile tends to be as the scheduled profile by the optimization model. Besides, the SoC of the battery (Fig. 25) has the same tendency as the expected SoC (Fig. 15).

Furthermore, the second frame of Fig. 18 presents the power profile exchanged with the utility. Once again, the profile is positive when microgrid sells power to the utility and negative when buys power. The behavior of this profile follows accurately the behavior expected in the optimization stage (see Fig. 7 and 8).

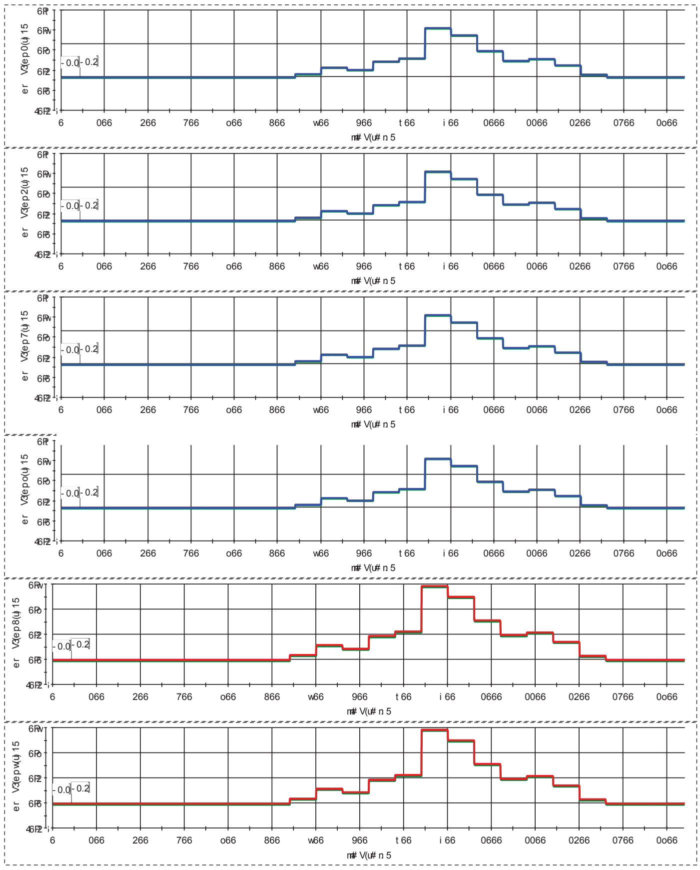

Fig. 21. Power profile of each PV array in real-time simulation considering scenario 2. Top to bottom: PV1 to PV6 power profiles. From PV1 to PV4: blue line: available power, green line: used power. For PV5 and PV6: red line: available power, green line: used power

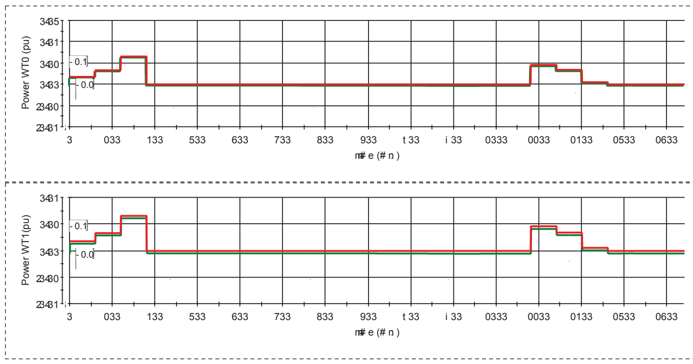

Fig. 22. Power profile of each WTs in real-time simulation considering scenario 2. Red line: available power, green line: used power

V. Conclusion and Future Works

A linear model for a grid-connected hybrid PV-Wind-Battery microgrid system has been proposed in order to minimize cost of buying energy from the grid and maximize profits for selling energy generated by PVs. The optimization strategy has been defined as a mixed integer lineal model to set optimal power references for the distributed resources of the microgrid. The strategy has been tested by considering two scenarios with different generation profiles. The behavior

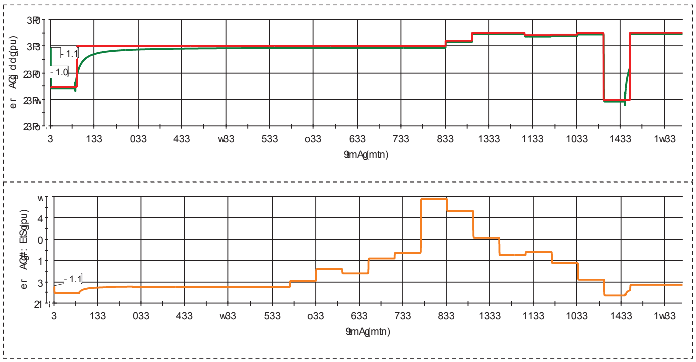

Fig. 23. Power profile of the battery and the utility in real-time simulation considering scenario 2. For battery power profile (top): scheduled profile (red line) and obtained profile (green line).

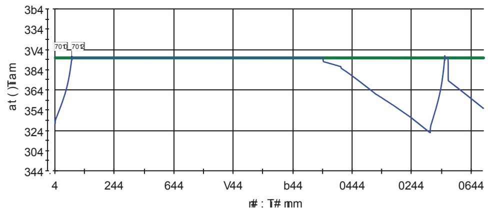

Fig. 24. Battery voltage obtained in real-time simulation considering scenario 2. Threshold voltage (green line) and battery voltage (blue line).

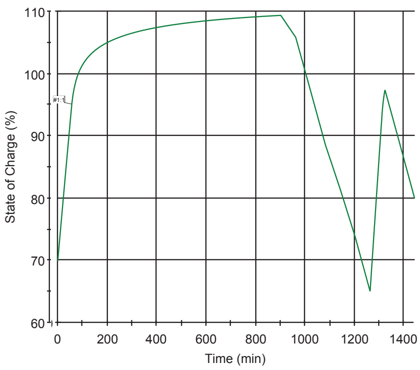

Fig. 25. SoC of the battery in real-time simulation considering scenario 2.

of the variables obtained in real-time simulation follows the expected features given by the optimization stage. As future work, demand side management should be considered to take advantage of the surplus renewable energy.

Acknowledgment

This work was supported by the Energy Technology Development and Demonstration Program through the Sino-Danish Project Microgrid Technology Research and Demonstration (www.meter.et.aau.dk).

References

[1] Microgrid technology research and demonstration. Aalborg University. [Online]. Available: www.meter.et.aau.dk

[2] M. Iqbal, M. Azam, M. Naeem, A. Khwaja, and A. Anpalagan, "Optimization classification, algorithms and tools for renewable energy: A review," *Renewable and Sustainable Energy Reviews*, vol. 39, no. 0, pp. 640 – 654, 2014.

[3] D. Wu, F. Tang, T. Dragicevic, J. Vasquez, and J. Guerrero, "Autonomous active power control for islanded ac microgrids with photovoltaic generation and energy storage system," *IEEE Transactions on Energy Conversion*, vol. 29, no. 4, pp. 882–892, Dec 2014.

[4] F. Katiraei, R. Iravani, N. Hatziargyriou, and A. Dimeas, "Microgrids management," *Power and Energy Magazine, IEEE*, vol. 6, no. 3, pp. 54–65, May 2008.

[5] I. S. C. C. 21, "Guide for optimizing the performance and life of lead-acid batteries in remote hybrid power systems," *IEEE Std 1561-2007*, pp. C1–25, 2008.

[6] F. Marra and G. Yang, "Decentralized energy storage in residential feeders with photovoltaics," in *Energy Storage for Smart Grids*, P. D. Lu, Ed. Boston: Academic Press, 2015, pp. 277 – 294.

[7] W. Shi, X. Xie, C.-C. Chu, and R. Gadh, "Distributed optimal energy management in microgrids," *IEEE Transactions on Smart Grid*, vol. 6, no. 3, pp. 1137–1146, May 2015.

[8] S. C. C. by letter Date: 2012-12-21. Shanghai region tariff table. [Online]. Available: http://www.sheitc.gov.cn/dfjf/637315.htm

[9] Intelligent microgrid laboratory. Aalborg University. [Online]. Available: http://www.et.aau.dk/department/laboratory-facilities/intelligent-microgrid-lab/